

FTO Coated Glass Electrode Functionalization with Transition Metal Cations Receptors via Electrostatic Self-Assembly

Szymon Jasiński¹, Justyna Czupryniak², Tadeusz Ossowski², Grzegorz Schroeder¹

¹ Faculty of Chemistry, Adam Mickiewicz University, Umultowska 89b, 61-614 Poznań, Poland

² Faculty of Chemistry, Gdańsk University, Sobieskiego 18, 80-952 Gdańsk, Poland

Received: 17 July 2013 / Accepted: 14 September 2013 / Published: 20 October 2013

Fabrication of new surface materials, FTO-coated glass electrode with electrostatic self-assembled monolayers of transition metal cations receptors, ferrozine and carboxylated porphine, is presented and described. Subsequent functionalization of electrode surface was confirmed by contact angle measurements as well as cyclic voltammetry study. The results show that desired modification was accomplished and complexed metal cations on the electrode surface were detected by cyclic voltammetry method.

Keywords: cyclic voltammetry, FTO, surface functionalization

1. INTRODUCTION

Functionalization of surface is a method of designing materials with desired properties. There are various chemical routes for altering the surface depending on its character. One of the most important is a self-assembled monolayer formation. Self-assembly is a commonly used method of surface properties modification such as surface energy, charge or polarity¹. The most commonly functionalized surfaces are noble metals for example gold modified with alkanethiols and sulfides²⁻⁵. Another group are surfaces terminated with hydroxyl groups as silica⁶⁻¹⁵ as well as metal oxides such as mixed indium tin oxide (ITO)¹⁶⁻³⁸ or fluorinated tin oxide (FTO)³⁹⁻⁴⁵ which are transparent conductive films deposited on glass substrates commonly used as electrodes. In case of silica and metal oxides surface the silanization method is widely used. The general formula of the applied compounds for this method is R—(CH₂)_n—Si—X₃ where R is an organofunctional group bounded to a silicon atom via alkyl chain linker. X is a hydrolyzable group (alkoxy, acyloxy, halogen or amine group). Such received thin films are stable because of a strong attachment to the surface through covalent bonding. Besides, the ease of the film fabrication and a variety of compounds usable for this

purpose result in wide application of this method to surface functionalization. Reactive functional groups of the anchored silanes allow further functionalization of such surfaces with desired compounds. Among interactions responsible for the multilayered thin films fabrication there are a covalent bound formation⁴⁶ for example via click chemistry⁴⁷, a coordinating bound formation⁴⁸ and an electrostatic interaction between oppositely charged molecules. This interaction plays basic role in the electrostatic self-assembly process of the multilayered thin films formation⁴⁹⁻⁵¹.

The aim of this work was an application of new surface materials obtained by modification of FTO coated glass electrode surface with ionic assemblies in electrochemical study of these materials. In this work the influence of FTO coated glass electrode functionalization, depending on the compounds used, on its response was studied by cyclic voltammetry. Surface modification was performed using two trialkoxysilanes with different alkyl chain length and molecular receptors complexing transition metal ions. Alkylsilanes used in this work are terminated with positive charged ammonium groups which are supposed to attract negatively charged receptor molecules equipped with carboxylic groups. Electrostatic self-assembly of multicharged small molecules leads to ordered thin ionic films due to dissipated charges on the whole molecule⁵². The analytical process occurs in the self-assembled monolayer (SAM) capable of complexing determined transition metal cations. Each step of the functionalization process was also determined by contact angle measurements, as the electrode surface hydrophobicity alters upon surface modification.

2. EXPERIMENTAL

2.1 FTO electrode preparation

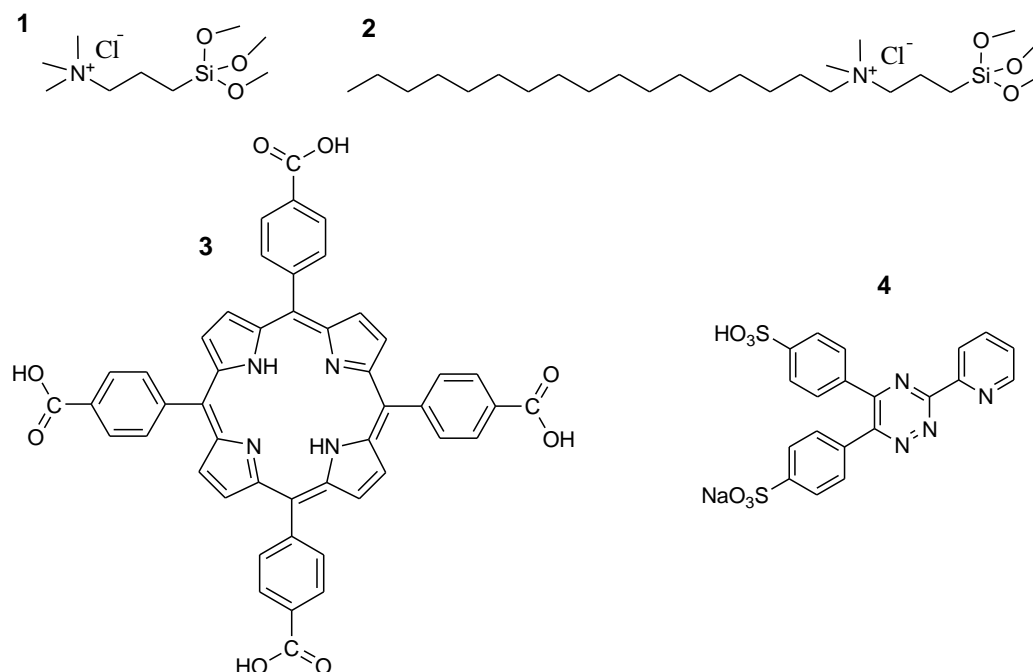


Figure 1. Compounds used for the functionalization of the FTO coated electrodes. 1 – TMATMS, 2-ODMATMS, 3-Porphine, 4-Ferrozine.

Compounds used for functionalization of the FTO electrodes are presented in the Fig. 1. The following silanes were used N-3-(Trimethoxysilyl)propyl-N,N,N-trimethylammonium chloride (**1** denoted as TMATMS) from ABCR GmbH and N-3-(Trimethoxysilyl)propyl-N-octadecyl-N,N-dimethylammonium chloride (**2** denoted as ODMATMS) from Aldrich. As the ion complexone, 4,4',4'',4'''-(Porphine-5,10,15,20-tetrayl)tetrakis(benzoic acid) (**3** denoted as Porphine) and 3-(2-pyridyl)-5,6-bis(4-phenylsulfonic acid)-1,2,4-triazine, monosodium salt (**4** known as Ferrozine) were used, both purchased from Aldrich.

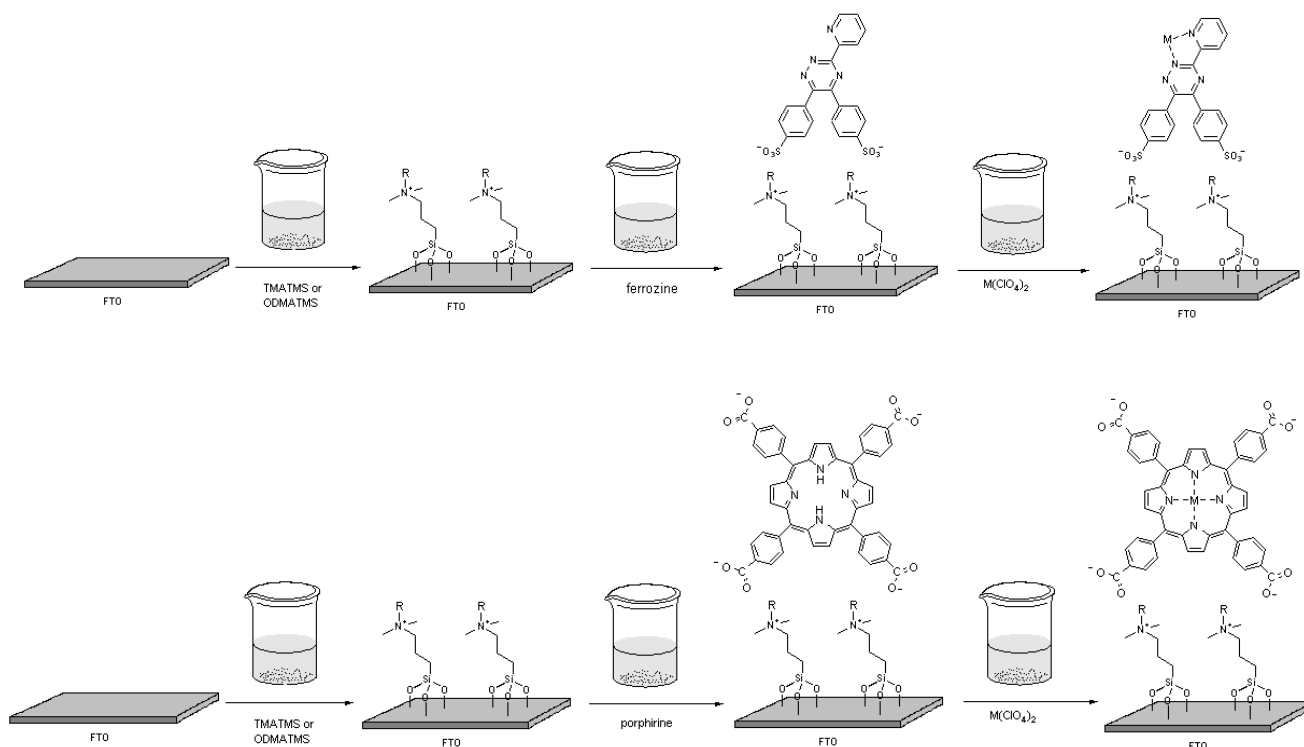


Figure 2. Functionalization of FTO coated electrodes with silanes R= CH₃ (TMATMS) or C₁₈H₃₇ (ODMATMS) and subsequent formation of electrostatic self-assembled films of **3** or **4**. The last step presents the metal – receptor complex formation where M= Fe²⁺ or Cu²⁺.

FTO coated glass purchased from Sigma Aldrich (surface resistivity ~ 7Ω/sq) was cut into 20x20mm sheets. Such prepared electrodes were cleaned in the ultrasonic bath in methanol, dried and subsequently immersed in 10⁻³ mol dm⁻³ of the silane **1** or **2** solutions in methanol for 24h. After washing and drying, FTO electrodes were carried to the 10⁻³ mol dm⁻³ aqueous solutions of **3** or **4**, previously converted into their sodium salts, for 15 min, washed and dried. In the next step functionalized FTO coated electrodes were immersed in aqueous solution of metal cations, Fe²⁺ and Cu²⁺ perchlorates respectively, for 15 min. Then the electrodes were rinsed in demineralized water and dried. The functionalization process is presented in Fig. 2. As prepared electrodes were used in cyclic voltammetry measurements.

2.2 Contact Angle measurements

Measurements were performed with the Krüss apparatus (DSA 100 Expert model) for automatic evaluation of contact angle and surface free energy as well as surface and interfacial tension by a droplet shape analysis. The device employs an optical method of contact angle evaluation. The measurements were carried out by the deposition of two water droplets onto each FTO sheet. The size of the droplet was 3 μl . For each the left and the right contact angle was measured and the resulting value is an arithmetic mean of both angles.

2.3 Voltammetry measurements

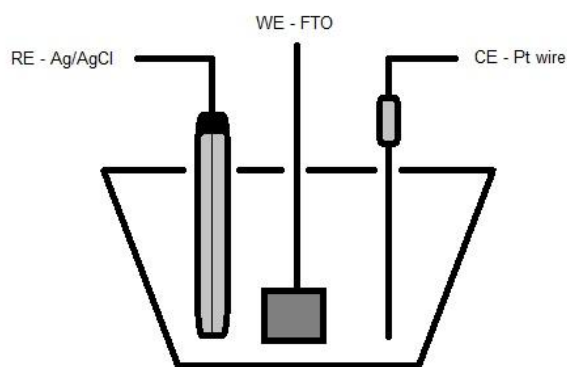


Figure 3. Scheme of cyclic voltammetry measurement system. Working electrode (WE) – functionalized FTO, counter electrode (CE) – Pt wire and reference electrode (RE) Ag/AgCl.

The electrochemical measurements were carried out in a single-compartment, three-electrode cell. The potential was applied with an Autolab potentiostat/galvanostat PGSTAT30 (Eco Chemie B.V., The Netherlands) controlled with General Purpose Electrochemical System (GPES 4.9) software. Platinum wire served as the counter electrode and a Ag/AgCl was used as the reference electrode. The voltammograms were obtained for clean FTO samples, after silanization process, electrostatic self-assembly of receptors and in the presence of transition metal cations (Fe^{2+} and Cu^{2+}). Scheme of the measuring system is presented in Fig. 3. The solutions consisted of a 0.1 mol dm^{-3} sodium perchlorate in water were used as a base electrolyte. All electrolyte solutions were purged with argon prior to use in an effort to remove oxygen from the solutions. Experiments were performed at room temperature (~ 24 °C). Voltammograms were scanned from $E=0\text{V}$ potential in the positive(anodic) direction at the scan rate of 0.1 Vs^{-1} .

3. RESULTS AND DISCUSSION

Contact Angle (CA) measurements of FTO electrodes were performed in order to confirm each step of functionalization process. Measured CA values are collected in the table 1. For bare FTO

electrode obtained CA value for the water droplet is 27.7°. A formation of silane monolayer onto FTO surface resulted in the CA value increase to 72.1° and 70.3° for TMATMS monolayer and ODMATMS monolayer respectively. Such an increment demonstrates a more hydrophobic character of the electrode surface which was expected after this step of functionalization.

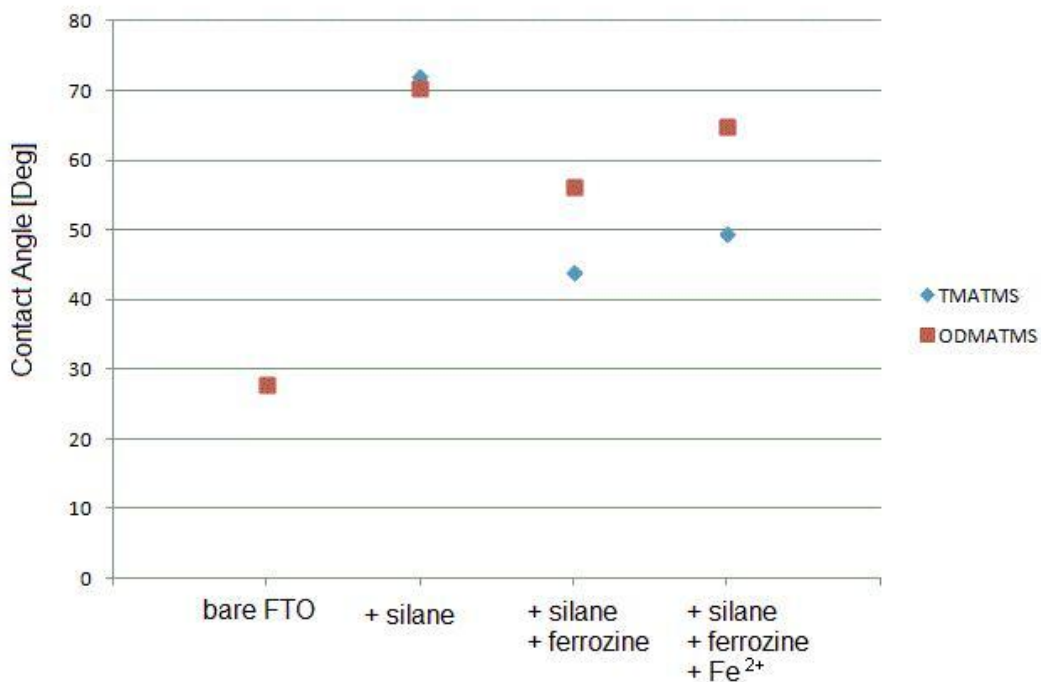


Figure 4. Contact angle measurements of bare FTO coated electrode and upon subsequent functionalization steps with ferrozine receptor used.

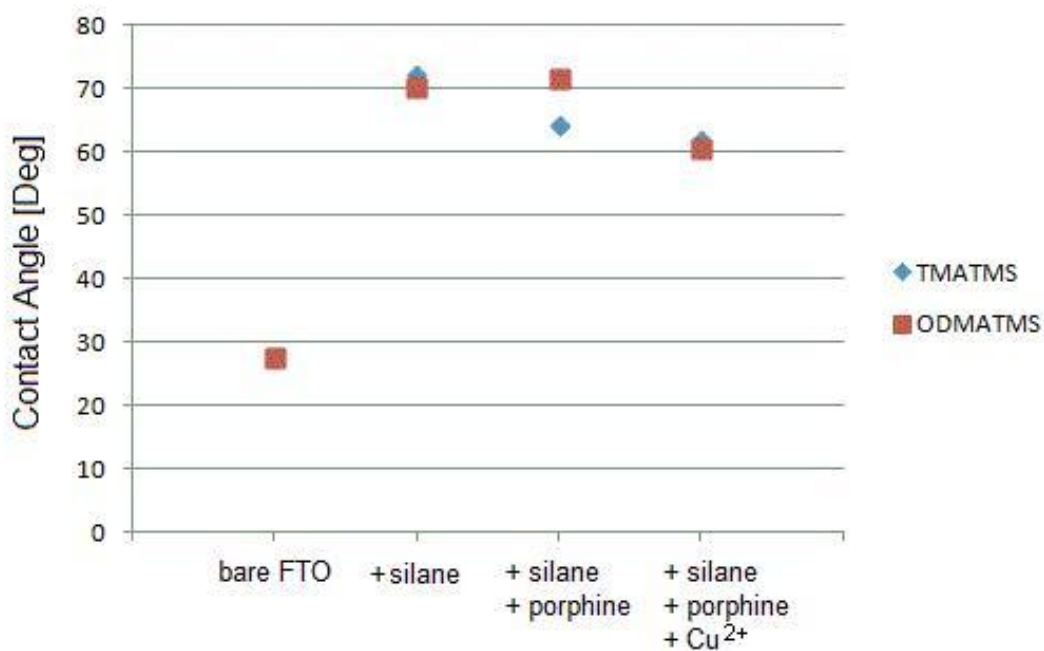


Figure 5. Contact angle measurements of bare FTO coated electrode and upon subsequent functionalization steps with porphine receptor used.

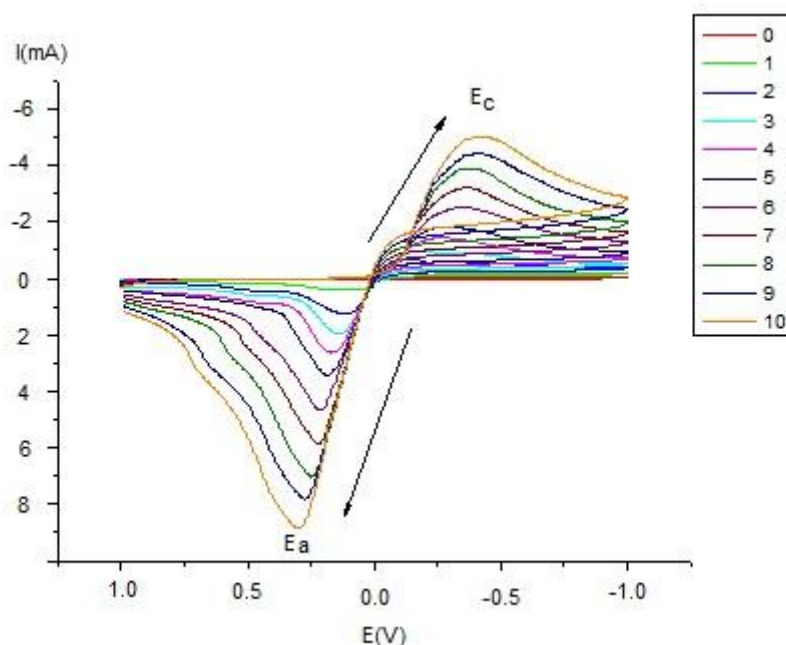


Figure 6. Voltammograms of the FTO electrode functionalized with ODMATMS and porphine electrostatic self-assembled monolayer (red). The Cu^{2+} ions influence on redox potentials alterations. The corresponding concentrations of Cu^{2+} ions are given in the table 3.

Within the next step of the surface modification receptor molecules were self-assembled as a result of electrostatic attraction. The CA measurements confirm this process with decreased values for both ferrozine and porphine receptors. In case of ferrozine the CA values are 44.0° for the TMATMS monolayer and 56.2° for the ODMATMS monolayer. For the porphine assembly resulting CA values are 64.3° and 71.7° for TMATMS and ODMATMS monolayer respectively. These minor differences can be explained with higher hydrophobicity of the porphine molecule than the ferrozine. After complexation of Fe^{2+} and Cu^{2+} cations the observed changes in CA values are slight and do not exceed 10° . The alterations of CA values due to FTO electrode functionalization are presented in Figures 4 and 5 (for Fe^{2+} and Cu^{2+} cations respectively) which show clearly that the surface hydrophobicity has changed.

Figure 6 presents voltammograms of the FTO-ODMATMS-porphine electrode in the presence of Cu^{2+} ions at concentrations given in the table 2. The influence of the increasing concentration of Cu^{2+} ions is observable by the altering redox potentials. The anodic potential E_a of $\text{Cu}^{0/2+}$ rises from 0.063 V at the concentration of $0.5 \times 10^{-4} \text{ mol dm}^{-3} \text{ Cu}^{2+}$ to 0.297 V at the concentration of $7.5 \times 10^{-4} \text{ mol dm}^{-3} \text{ Cu}^{2+}$. The cathodic potential E_c of $\text{Cu}^{0/2+}$ changes the similar way from -0.147 V at the concentration of $0.5 \times 10^{-4} \text{ mol dm}^{-3} \text{ Cu}^{2+}$ to -0.416 V at the concentration of $7.5 \times 10^{-4} \text{ mol dm}^{-3} \text{ Cu}^{2+}$. The difference between E_a and E_c (ΔE) increases from 0.210 V at the first concentrations of Cu^{2+} ions measured to 0.713 V at the last concentration.

The first curve (red) corresponds to FTO-ODMATMS-Porphine functionalized electrode in the absence of Cu^{2+} ions. There are cathodic potential $E_c = -0.577 \text{ V}$ and anodic potential $E_a = -0.338 \text{ V}$

present of relatively low current intensities. They are associated with the redox process of the porphine molecules electrostatically self-assembled onto electrode surface.

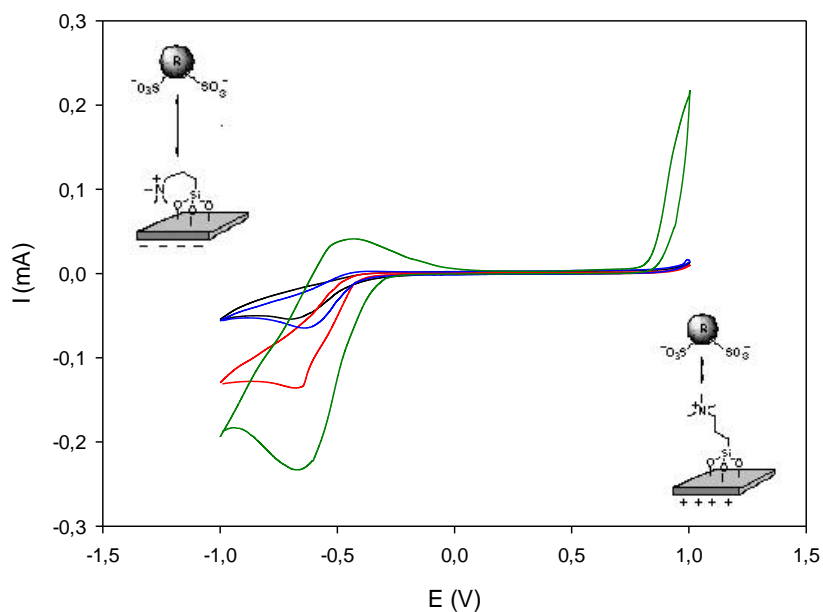


Figure 7. Cyclic voltammograms of the following functionalization steps of FTO coated glass electrodes in 0,1M NaClO₄ with scan rate of 0,1Vs⁻¹ vs Ag/AgCl. Bare electrode (black), TMATMS monolayer (red), TMATMS-ferrozine layer (blue) and TMATMS-ferrozine with Fe²⁺ ions complexed (green).

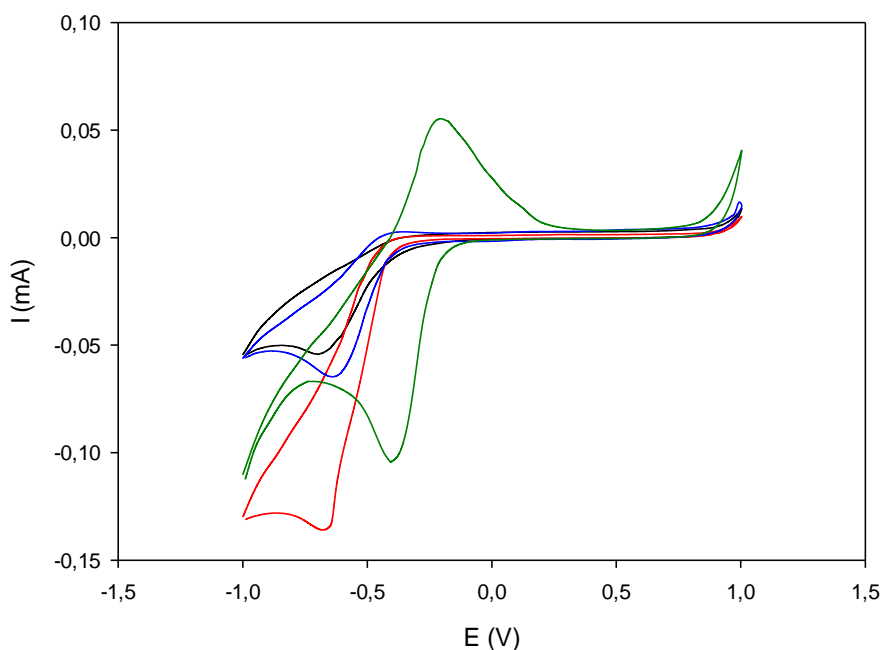


Figure 8. Cyclic voltammograms of the following functionalization steps of FTO coated glass electrodes in 0,1M NaClO₄ with scan rate of 0,1Vs⁻¹ vs Ag/AgCl. Bare electrode (black), TMATMS monolayer (red), TMATMS-ferrozine layer (blue) and TMATMS-ferrozine with Cu²⁺ ions complexed (green).

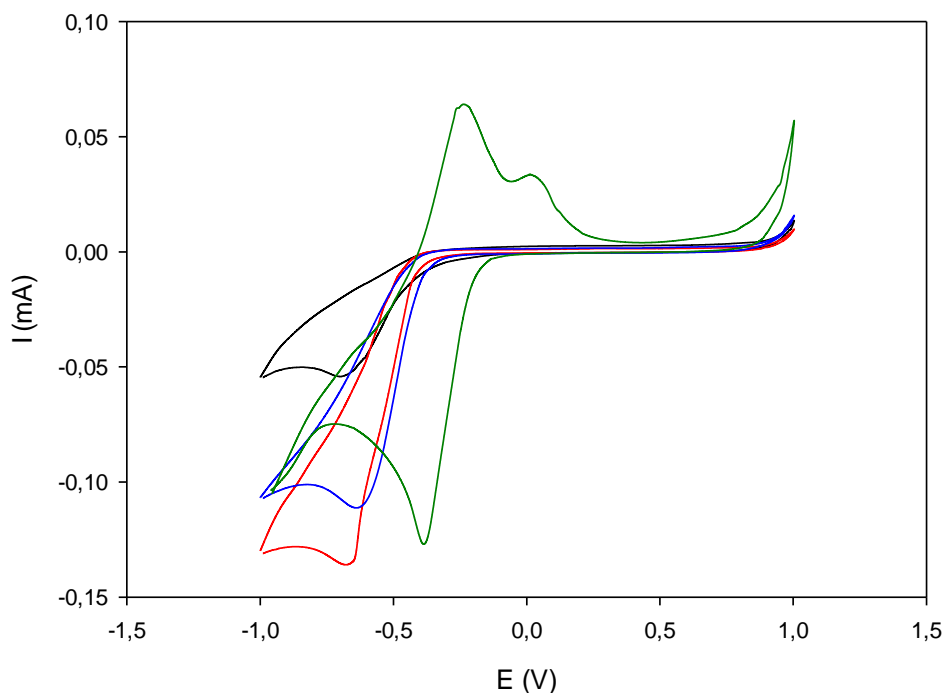


Figure 9. Cyclic voltammograms of the following functionalization steps of FTO coated glass electrodes in 0,1M NaClO₄ with scan rate of 0,1Vs⁻¹ vs Ag/AgCl. Bare electrode (black), TMATMS monolayer (red), TMATMS-porphine layer (blue) and TMATMS-porphine with Cu²⁺ ions complexed (green).

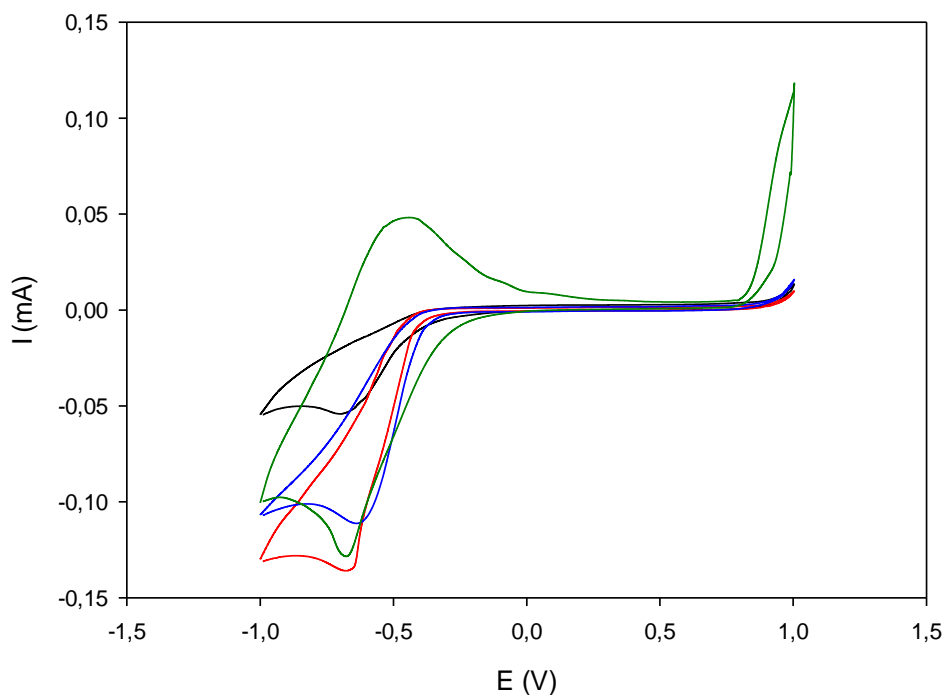


Figure 10. Cyclic voltammograms of the following functionalization steps of FTO coated glass electrodes in 0,1M NaClO₄ with scan rate of 0,1Vs⁻¹ vs Ag/AgCl. Bare electrode (black), TMATMS monolayer (red), TMATMS-porphine layer (blue) and TMATMS-porphine with Fe²⁺ ions complexed (green).

Figures 7-14 present a comparison of cyclic voltammograms for each silane-receptor-cation system measured depending on the functionalization step of the electrode.

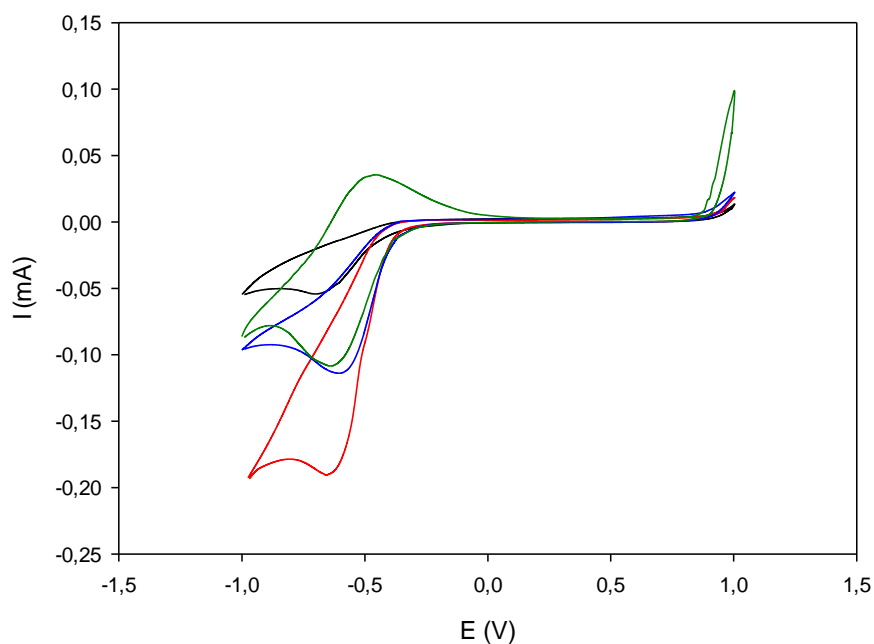


Figure 11. Cyclic voltammograms of the following functionalization steps of FTO coated glass electrodes in 0,1M NaClO_4 with scan rate of $0,1\text{Vs}^{-1}$ vs Ag/AgCl. Bare electrode (black), ODMATMS monolayer (red), ODMATMS-ferrozine layer (blue) and ODMATMS-ferrozine with Fe^{2+} ions complexed (green).

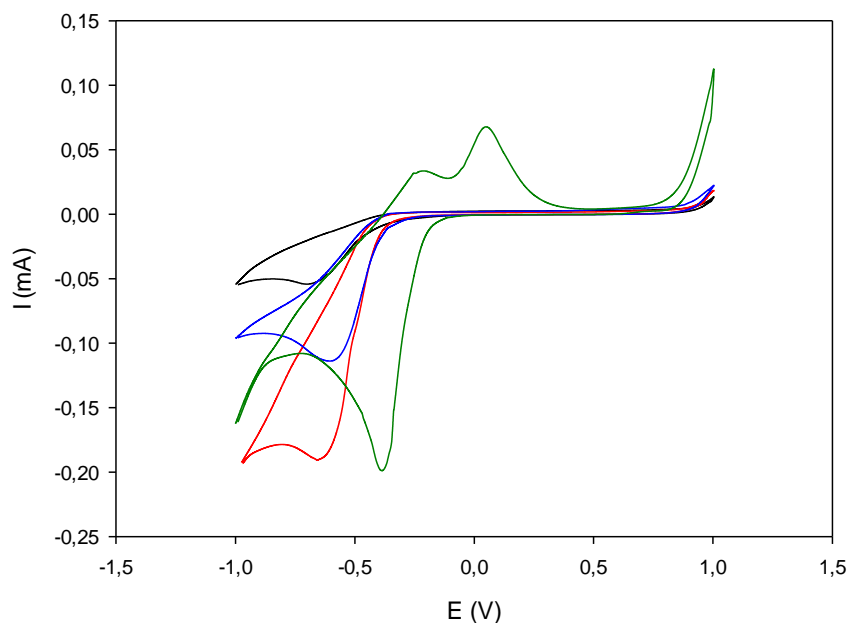


Figure 12. Cyclic voltammograms of the following functionalization steps of FTO coated glass electrodes in 0,1M NaClO_4 with scan rate of $0,1\text{Vs}^{-1}$ vs Ag/AgCl. Bare electrode (black), ODMATMS monolayer (red), ODMATMS-ferrozine layer (blue) and ODMATMS-ferrozine with Cu^{2+} ions complexed (green).

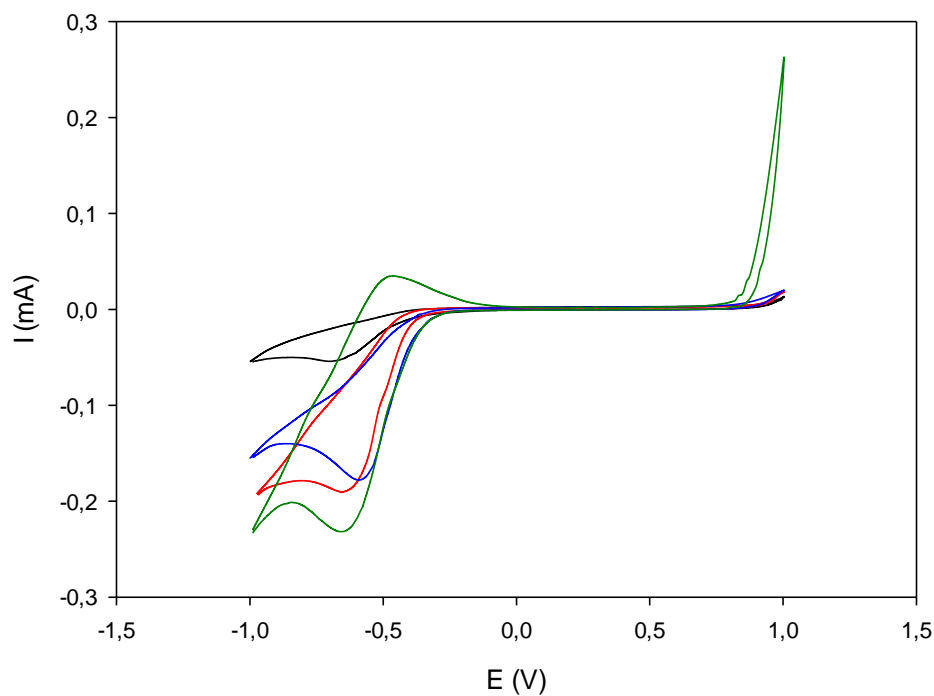


Figure 13. Cyclic voltammograms of the following functionalization steps of FTO coated glass electrodes in 0,1M NaClO₄ with scan rate of 0,1Vs⁻¹ vs Ag/AgCl. Bare electrode (black), ODMATMS monolayer (red), ODMATMS-porphine layer (blue) and ODMATMS- porphine with Fe²⁺ ions complexed (green).

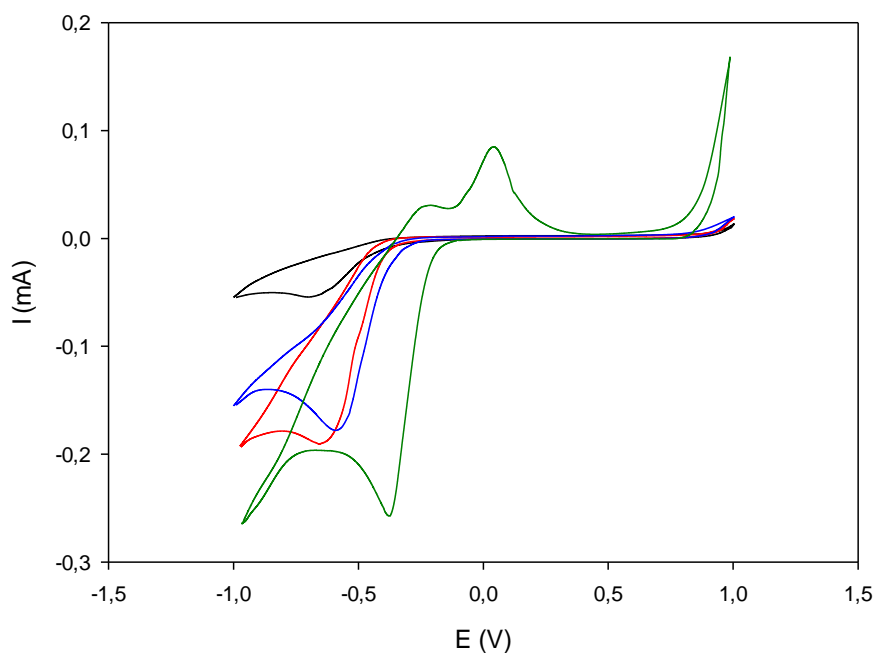


Figure 14. Cyclic voltammograms of the following functionalization steps of FTO coated glass electrodes in 0,1M NaClO₄ with scan rate of 0,1Vs⁻¹ vs Ag/AgCl. Bare electrode (black), ODMATMS monolayer (red), ODMATMS-porphine layer (blue) and ODMATMS- porphine with Cu²⁺ ions complexed (green).

For electrodes with complexed metal cations on the surface, there are noticeable redox peaks on the recorded voltammograms. The oxidation/reduction potentials of the measured systems are collected in the table 3. The voltammograms of the electrodes with complexed Fe^{2+} cation show anodic potential of -0.455 V for ferrozine as a receptor molecule as well as -0.466 V and -0.481 V for porphine as a receptor molecule on the FTO electrode functionalized with TMATMS and ODMATMS respectively.

Cathodic potential for the ferrous cation varies from -0.623 V and -0.645 V for ferrozine containing electrodes to -0.655 V and -0.660 V for porphine containing electrodes.

Table 1. Contact angle measured for each functionalization step of FTO coated electrode.

Functionalization step	Contact Angle [Deg]	
	TMATMS	ODMATMS
Bare FTO	27.7	27.7
FTO-silane	72.1	70.3
FTO-silane-ferrozine	44.0	56.2
FTO-silane-ferrozine- Fe^{2+}	49.4	64.8
FTO-silane-porphirine	64.3	71.7
FTO-silane-porphirine- Cu^{2+}	61.8	60.6

Table 2. The redox process parameters of the FTO electrode functionalized with ODMATMS and a porphine electrostatic self-assembled monolayer in the presence of Cu^{2+} ions.

No.	Cu^{2+} [mol dm^{-3}]	E_c [V]	E_a [V]	E_{c2} [V]	ΔE [V]
0	0	-0.577	-0.338	-	0.239
1	0.5×10^{-4}	-0.147	0.063	-0.528	0.210
2	1.0×10^{-4}	-0.128	0.102	-0.445	0.230
3	1.5×10^{-4}	-0.182	0.131	-0.323	0.313
4	2.0×10^{-4}	-0.245	0.170	-	0.415
5	2.5×10^{-4}	-0.255	0.185	-	0.440
6	3.5×10^{-4}	-0.328	0.209	-	0.537
7	4.5×10^{-4}	-0.367	0.219	-	0.586
8	5.5×10^{-4}	-0.382	0.248	-	0.630
9	6.5×10^{-4}	-0.411	0.273	-	0.684
10	7.5×10^{-4}	-0.416	0.297	-	0.713

These potentials values correspond to $\text{Fe}^{0/2+}$ reduction/oxidation process of complexed iron cations. In case of the electrodes with Cu^{2+} cations complexed, voltammograms show two anodic peaks except of the FTO-TMATMS-ferrozine- Cu^{2+} system, where the second anodic peak is absent. The first anodic peak potential was observed at -0.208 V and -0.213 V for the ferrozine containing electrodes

functionalized with TMATMS and ODMATMS respectively. In case of the porphine containing electrodes a 0.026 V shift of this peak in the negative direction was noticed resulting in the potential -0.234 V for FTO-TMATMS-porphine and -0.239 V for FTO-ODMATMS-porphine. The second anodic peak potential was observed at 0.055 V for FTO-ODMATMS-ferrozine and at 0.029 V and 0.045 V for porphine containing electrodes functionalized with TMATMS and ODMATMS respectively. The cathodic peak potential for the cupric cation was observed at -0.397 V and -0.387 V for ferrozine containing FTO electrode functionalized with TMATMS and ODMATMS respectively. In case of porphine containing electrodes these potentials were observed at -0.381 V and -0.397 V. These potentials values correspond to $\text{Cu}^{0/2+}$ reduction/oxidation process of complexed copper ions.

Table 3. Redox potentials of the measured functionalized electrodes depending on a silane, a receptor molecule and a transition metal cation used in 0,1M NaClO_4 at the scan rate of 0.1 Vs^{-1} .

FTO functionalized electrode system	Cation				
	Fe^{2+}		Cu^{2+}		
	E_a	E_c	E_{a1}	E_{a2}	E_c
FTO-TMATMS-F	-0.455 V	-0.645 V	-0.208 V	-	-0.397 V
FTO-TMATMS-P	-0.466 V	-0.660 V	-0.234 V	0.029 V	-0.381 V
FTO-ODMATMS-F	-0.455 V	-0.623 V	-0.213 V	0.055 V	-0.387 V
FTO-ODMATMS-P	-0.481 V	-0.655 V	-0.239 V	0.045 V	-0.397 V

In this work we have fabricated FTO/TMATMS and FTO/ODMATMS functionalized electrodes. Both systems possess positively charged ammonium group, which is vulnerable to the potential applied to the electrode. When the potential is negative, ammonium group is attracted to the electrode surface and the distance between this group and oppositely charged receptor molecule is increased. Whenever the potential becomes positive this ammonium group begins to be repulsed from the electrode surface and the distance between this group and the receptor molecule is decreased. This effect (illustrated in Fig. 7) needs to be taken into account while discussing the electrochemical response of the electrode. Movement of the ionic layer on the functionalized FTO surface during the potential switching results in absence of a stable electric double layer, contrary to metal electrodes. Furthermore, the ionic SAM movement under the potential alteration differentiates the electrode working conditions both within positive and negative potential which influences the analyte redox potentials.

4. CONCLUSION

FTO coated glass electrodes were functionalized with alkylsilane monolayers and subsequently electrostatic self-assembled layer of transition metal cation receptors was formed. Then the metal

cations were complexed on the electrode surface and the contact angle as well as cyclic voltammetry measurements were performed. CA values obtained corroborate with each step of the functionalization process accomplished. Electrochemical measurements also confirmed the following steps of the FTO electrode modification as well as the presence of the Cu^{2+} and Fe^{2+} cations. In this work we present simple and effective technique of FTO-coated glass electrode functionalization with molecular receptors for transition metal cations. This method allows a wide spectrum of molecules to be self-assembled on such electrodes as the electrostatic self-assembly is a facile route to achieve a monolayer with desired analytical properties.

References

1. A. Ulman, *An Introduction to Ultra Thin Films from Langmuir-Blodgett to Self-Assembly*, Academic Press, London, (1991)
2. Y. Sato, K. Uosaki, *J. Electroanal. Chem.*, 384 (1995) 57
3. T. Kondo, M. Takechi, Y. Sato, K. Uosaki, *J. Electroanal. Chem.*, 381 (1995) 203
4. Y. Hou, S. Helali, A. Zhang, N. Jaffrezic-Renault, C. Martelet, J. Minic, T. Gorojankina M.-A. Persuy, E. Pajot-Augy, R. Salesse, F. Bessueille, J. Samitier, A. Errachid, V. Akimow, L. Reggiani, C. Pennetta, E. Alfinito, *Biosensors and bioelectronics*, 21 (2006) 1393
5. R. Shabani, S.A. Mozaffari, S.W. Husain, M. S. Tehrani, *Iran. J. Sci. Technol.*, 33 (2009) 335
6. J. F. Mooney, A. J. Hunt, J. R. McIntosh, C. A. Liberko, D. M. Walba, C. T. Rogers, *Proc. Natl. Acad. Sci.*, 93 (1996) 12287
7. A. K. Chauhan, D. K. Aswal, S. P. Koiry, S. K. Gupta, J. V. Yakhmi, C. Sügers, D. Guerin, S. Lenfant, D. Vuillaume, *Appl. Phys. A*, 90 (2008) 581
8. S. A. Kulkarni, S. B. Ogale, K. P. Vijayamohanam, *J. Colloid Interf. Sci.*, 318 (2008) 372
9. R. Soler, J. Salabert, R. M. Sebastian, A. Vallribera, N. Roma, S. Ricart, E. Molins, *Chem. Commun.*, 47 (2011) 2889
10. K. Yu, W. Sommer, J. M. Richardson, M. Weck, C. W. Jones, *Adv. Synth. Catal.*, 347 (2005) 161
11. S. J. Lee, D. R. Bae, W. S. Han, S. S. Lee, J. H. Jung, *Eur. J. Inorg. Chem.*, 10 (2008) 1559
12. F. Da Cruz, K. Driaf, C. Berthier, J.-M. Lameille, F. Armand, *Thin Solid Films*, 349 (1999) 155
13. E. J. Cho, S. Jung, K. Lee, H. J. Lee, K. C. Nam, H.-J. Bae, *Chem. Commun*, 46 (2010) 6557
14. R. Chen, R. P. J. Bronger, P. C. J. Kamer, P. W. N. M. van Leeuwen, J. N. H. Reek, *J. Am. Chem. Soc.*, 126 (2004) 14557
15. P. Teolato, E. Rampazzo, M. Arduini, F. Mancin, P. Tecilla, U. Tonellato, *Chem. Eur. J.*, 13 (2007) 2238
16. Z. B. Zhang, S. J. Yuan, X. L. Zhu, K. G. Neoh, E. T. Kang, *Biosensors and Biochemicals*, 25 (2010) 1102
17. L. Valentini, M. Cardiani, J. M. Kenny, *Carbon*, 48 (2010) 861
18. S. E. Koh, K. D. McDonald, D. H. Holt, C. S. Dulcey, *Langmuir*, 22 (2006) 6249
19. E. J. Moore, M. Curtin, J. Ionita, A. R. Maguire, G. Ceccone, P. Galvin, *Anal. Chem.*, 79 (2007) 2050
20. S. S. Shah, M. Kim, E. Foster, T. Vu, D. Patel, L.-J. Chen, S. V. Verkhoturov, E. Schweikert, G. Tae, A. Revzin, *Anal. Bioanal. Chem.*, 402 (2012) 1847
21. M. Khalid, N. Wasio, T. Chase, K. Bandyopadhyay, *Nanoscale Res. Lett.*, 5 (2010) 61
22. M. Khalid, I. Pala, N. Wasio, K. Bandyopadhyay, *Colloid. Surface. A*, 348 (2009) 263
23. X. Liu, K. G. Neoh, E. T. Kang, *Langmuir*, 18 (2002) 9041
24. H. Hillebrandt, M. Tanasaka, *J. Phys. Chem. B*, 105 (2001) 4270
25. H. Wei, J. Li, Y. Wang, E. Wang, *Nanotechnology*, 18 (2007) 175610

26. K. Ariga, K. Tanaka, K. Katagiri, J. Kikuchi, H. Shimakoshi, E. Ohshima, Y. Hisaeda, *Phys. Chem. Chem. Phys.*, 3 (2001) 3442
27. M. Miyachi, M. Ohta, M. Nakai, Y. Kubota, Y. Yamanoi, T. Yonezawa, H. Nishihara, *Chem. Lett.*, 37 (2008) 404
28. R. Schlapak, D. Armitage, N. Saucedo-Zeni, M. Hohage, S. Howorka, *Langmuir*, 23 (2007) 10244
29. S. Besbes, H. Ben Ouada, J. Davenas, L. Ponsonnet, N. Jaffrezic, P. Alcouffe, *Mater. Sci. Eng.*, 26 (2006) 505
30. S. Besbes, A. Ltaief, K. Reybier, L. Ponsonnet, N. Jaffrezic, J. Davenas, H. Ben Ouada, *Synthetic Met.*, 138 (2003) 197
31. I. Markovich, D. Mandler, *J. Electroanal. Chem.*, 500 (2001) 453
32. G. Zotti, A. Randi, S. Destri, W. Porzio, G. Schiavon, *Chem. Mater.*, 14 (2002) 4550
33. A. Muthurasu, V. Ganesh, *J. Colloid Interf. Sci.*, 374 (2012) 241
34. D. Wu, J. Liu, Y. Wang, *Appl. Surf. Sci.*, 256 (2010) 2934
35. J. Lee, B.-J. Jung, J.-I. Lee, H. Y. Chu, L.-M. Do, H.-K. Shim, *J. Mater. Chem.*, 12 (2002) 3494
36. J. Xu, J.-J. Zhu, Y. Zhu, K. Gu, H.-Y. Chen, *Anal. Lett.*, 34 (2001) 503
37. R. A. Hatton, S. R. Day, M. A. Chesters, M. R. Willis, *Thin Solid Films*, 394 (2001) 292
38. C.-G. Wu, H.T. Hsiao, Y.-R. Yeh, *J. Mater. Chem.*, 11 (2001) 2287
39. B.-X. Lei, J.-Y. Liao, RT. Zhang, J. Wang, C.-Y. Su, D.-B. Kuang, *J. Phys. Chem.*, 114 (2010) 15228
40. A. Fattori, L. M. Peter, K. L. McCall, N. Robertson, F. Marken, *J. Solid State Electrochem.*, 14 (2010) 1929
41. K.-S. Tseng, L.-C. Chen, K.-C. Ho, *Sensors and Actuators B*, 108 (2005) 738
42. C. Sima, C. Grigoriu, S. Antohe, *Thin Solid Films*, 519 (2010) 595
43. R. Valaski, C. D. Canestraro, L. Micaroni, R.M.Q. Mello, L.S. Roman, *Solar Energy Materials & Solar Cells*, 91 (2007) 684
44. S. Sakurai, H.-Q. Jiang, M. Takahashi, K. Kobayashi, *Electrochimica Acta*, 54 (2009) 5463
45. P. Chatchai, S. Kishioka, Y. Murakami, A.Y. Nosaka, Y. Nosaka, *Electrochimica Acta*, 55 (2010) 592
46. P. Kohli, K. K. Taylor, J. J. Harris, G. J. Blanchard, *J. Am. Chem. Soc.*, 120 (1998) 11962
47. G. K. Such, J. F. Quinn, A. Quinn, E. Tjipto, F. Caruso, *J. Am. Chem. Soc.*, 128 (2006) 9318
48. H. Lee, L. J. Kepley, H. G. Hong, T. E. Mallouk, *J. Am. Chem. Soc.*, 110 (1988) 618
49. G. Decher, J. D. Hong, *Makromol. Chem. Macromol. Symp.*, 46 (1991) 321
50. G. Decher, J. D. Hong, *Ber. Bunsen-Ges. Phys. Chem.*, 95 (1991) 1430
51. G. Decher, J. D. Hong, J. Schmitt, *Thin Solid Films*, 210 (1992) 831
52. S. Jasiocki, J. Serafińczuk, T. Gotszalk, G. Schroeder, *J. Nanomater.*, (2012) art. no. 568326